IEEE Access
Multidisciplinary : Rapid Review : Open Access Journal

Received 19 April 2024, accepted 30 April 2024, date of publication 9 May 2024, date of current version 24 May 2024.

Digital Object Identifier 10.1109/ACCESS.2024.3399563

RESEARCH ARTICLE

Empowering Energy-Sustainable IoT Devices With Harvest Energy-Optimized Deep Neural Networks

SAEED ALZAHRANI[1], (Member, IEEE), ADEB SALH[2], LUKMAN AUDAH[3], (Member, IEEE), MOHAMMED A. ALHARTOMI[1], (Member, IEEE), ABDULAZIZ ALOTAIBI[4], AND RUWAYBIH ALSULAMI[5], (Member, IEEE)

[1]Department of Electrical Engineering, University of Tabuk, Tabuk 71491, Saudi Arabia
[2]Faculty of Information and Communication Technology, Universiti Tunku Abdul Rahman (UTAR), Kampar, Perak 31900, Malaysia
[3]Faculty of Electrical and Electronic Engineering, Universiti Tun Hussein Onn Malaysia, Parit Raja 86400, Malaysia
[4]Department of Industrial Engineering, University of Tabuk, Tabuk 71491, Saudi Arabia
[5]Department of Electrical Engineering, Umm Al-Qura University, Makkah 24382, Saudi Arabia

Corresponding authors: Mohammed A. Alhartomi (malhartomi@ut.edu.sa) and Adeb Salh (adebali@utar.edu.my)

The authors extend their appreciation to the Deputyship for Research & Innovation, Ministry of Education in Saudi Arabia for funding this research work through project number (S-1443-0183).

ABSTRACT There is a growing demand for low-power network devices; therefore, enabling technologies for the Internet of Things (IoT) is significantly important. This paper proposed resource allocation by maximizing the harvested energy to substantially improve Energy Efficiency (EE) and regulate transmission power for the scheduled IoT devices. Energy Harvesting (EH) is a viable technology that enables long-term and self-sustainable operations for IoT devices. The Simultaneous Wireless Information and Power Transfer (SWIPT) has been proposed as a promising solution for maximizing EE while ensuring the quality of service of all IoT devices, where the ultra-low power devices harvest energy in Power Splitting (PS) mode. This paper applied the proposed Optimal Transmit Power and PS Ratio (OTPR) algorithm to maximize the EE for SWIPT based on the partial derivative of Lagrange dual decomposition methods. The algorithm jointly optimized the allocation of the channel, PS, and power control to solve the distributed non-convex and NP-hardness caused by co-channel interference. A novel training was proposed for Deep Neural Network (DNN) algorithms chain rules to minimize the loss function based on updating the parameters of the weights hidden layer and convergence training to achieve near-optimal performance and minimize unneeded label data. The simulation results showed that the DNN training for the chain rule provided a near-optimal performance EE with the shortest training time. This observation indicated that decreasing the loss function at every training optimizes the co-channel conditions for IoT devices by assigning the EH requirement to meet the minimum harvesting need.

INDEX TERMS Internet of Things, energy efficiency, power splitting, deep neural network, energy harvesting.

I. INTRODUCTION

Recent developments in information technology have increased the number of wireless devices used for interaction and communication connected to the Internet of Things (IoT) devices. The development of 500 billion smart wireless devices is expected in future IoT applications [1].

Two main issues are the power consumption and the short battery life of cellular connectivity for IoT [2]. With renewable energy sources, Energy Harvesting (EH) technology has gained significant interest in the IoT. As more devices share the same wireless resources, mutual interference reduction and energy-efficient Resource Allocation (RA) in EH are investigated for a fully sustainable cooperative IoT network. The RA in EH radio and other EH systems has been a hot area of study from the perspective of green communication. Modern wireless networks must use RA strategies to

The associate editor coordinating the review of this manuscript and approving it for publication was Yeon-Ho Chung.

decrease the computing complexity of the power control for large interference channels and energy arriving at unexpected times. Much research has been devoted to the RA domain in EH and the battery life for wireless devices to minimize the cost and maximize Energy Efficiency (EE) performance. IoT devices' size and space restrictions significantly affect the battery life, and replacing batteries is expensive and can adversely impact the environment [3], [4]. The wireless EH technology is a versatile technique that can provide stable and sustained energy and a prolonged lifetime of energy-constrained networks; thus, it has attracted massive attention for IoT applications. For efficient IoT devices, Simultaneous Wireless Information and Power Transfer (SWIPT) is emerging as a promising technique that enables the continuous operation of low-power and data-hungry networks to support the sustainable operation of IoT devices. The SWIPT uses Radio Frequency (RF) signals to achieve dual functions of Information Decoding (ID) and EH [5]. Achieving an energy-sustainable IoT via SWIPT depends on Power Splitting (PS), which coordinates the EH circuits and information processes from RF signals to power the IoT device's requirement to be effectively handled [6]. Moreover, the SWIPT in a multi-antenna Transmitter (TX) has a significant potential to restore depleted energy continuously.

A major challenge of EH in IoT is that the harvested energy may be unpredictable and varying due to the stochastic nature of energy sources in the environment. Consequently, the IoT will consume additional energy for mobile and IoT devices with a limited battery capacity. EH can extend the lifetime of energy-constrained wireless devices from external renewable sources such as solar, wind, light, heat, and RF; thus, the EH offers a potential energy solution for IoT applications [2], [7].

A. RELATED WORK

Several emerging Beyond Fifth Generation (B5G) technologies have been deployed recently to improve further the EE transmission of an EH-enabled IoT network supported by SWIPT to assist a fully sustainable network. Channel assignment and Power Allocation (PA) have been proposed to improve the transmission power connected to the same channel to guarantee Quality of Service (QoS) to IoT devices [8]. The authors in [9] examined RF-EH and Non-Orthogonal Multiple Access (NOMA)-based information transmission with interference signals for the IoT that frequently caused a loss of system rate. In addition, the research maintained interference minimization and a sufficient energy supply for reliable and successful communications between devices. The interference can be an additional power source for RF-based EH to charge IoT devices to minimize the power control for wide interference channels. However, the authors in [10] studied the K-user interference channel with EH constraints and the Deep Neural Networks (DNN)-based RA method to maximize the sum rate. The DNN is acknowledged as a potent deep-learning paradigm for resolving a wide range of issues with IoT and wireless network systems. DNN has opened up a wide range of intriguing applications in wireless communications due to its accuracy in estimating high nonlinear functions at minimal complexity. Interestingly, this rapid expansion of IoT creates its own set of sustainability issues, mostly because of the higher maintenance requirements and energy requirements for both charging IoT devices and processing and storing vast amounts of IoT data in data and computing centers. Maintaining the high QoS in EH systems is challenging due to the unpredictable nature of RE quality, which hinders the effective energy conservation for IoT. The DNN-DRL method accurately determines the optimal strategy for forecasting RE. Enhancing IoT device processing, the method extends the system state to anticipated experiences for each time slot based on the anticipated amount of RE to store extra energy during times of abundance and use it during increased demand. This proposed method could reduce computational complexity based on controls of the transmit power and PS ratio and decrease the training failures induced by the conventional deep learning method. However, authors in [11] obtained the optimal transmit power in distributed antenna system-based SWIPT, which can be a sustainable solution for EE maximization in ultra-low power devices that harvest energy in PS. To reduce the computational time and increase the performance evaluation for the RF-EH IoT system, the authors in [11] suggested an approach based on the Lagrangian multiplier method that improved the convergence rate to discover the ideal solution without iterative computation. The EH, PS, and transmit power limitations examined the algorithm. IoT devices may now use energy more efficiently because of recent developments in EH technology, such as enhanced solar EH and new RF EH techniques. Performance is maintained while energy reductions are facilitated by advanced power management such as voltage a frequency scaling dynamically. Because automation streamlines processes, can focus on energy management solutions. DNN-based solutions are crucial to maximizing EH, optimizing energy consumption, and promoting preventive maintenance all of which help the sustainability of the IoT. Decentralized DNN systems enable cooperative training amongst IoT devices while reducing transmission overhead and ensuring data privacy. The dynamics of the harvested energy must be handled by resolving concerns for EH-based wireless communication systems [12]. Developing the rate energy performance of Multiple Input Single Output (MISO)-SWIPT systems based on making a good trade-off between received power for EH and data transmission is crucial for improving the transmission efficiency and EH efficiency [13]. The minimization of TX power needs to satisfy QoS and EH requirements, and optimization of TX precoding and PS operation depends on the need of RXs to complete ID and EH [14]. Increasing the lifetime of the RF-EH IoT system with QoS requirements is important to optimize the minimum harvested energy among RXs, depending on achieving an optimal TX precoding and designing the IoT PS [15].

Moreover, the global optimal TX precoding and RX-PS operation are involved in realistic nonlinear RF-EH modeling in SWIPT systems; they are still unknown for energy-sustainable multiuser MISO in IoT [16]. Due to the non-convexity created due to large interference channels, the authors [16] proposed an RA method based on deep learning that sought to maximize EE for SWIPT using PS mode with EH. Many works have aimed to enhance energy-sustainable IoT by proposing DNN learning for SWIPT to optimize transmit-harvest-powered interference channels to solve the non-convex optimization problem and maximize the energy-efficient RA in IoT devices [17], [18], [19], [20], [21]. The authors in [19] and [21] presented RA based on supervised learning on a DNN to approximate the Weighted Minimal Mean Square Error (WMMSE), a suitable method of PA for the interference channel. It has been demonstrated that the DNN can converge the behavior of the WMMSE method to achieve a data rate with less computing complexity. Authors in [20] suggested a dual-mode-SWIPT with intelligent splitting based on DNN learning. The duty-cycling method was developed for self-powering based on the nonlinear EH model to maximize a feasible rate under the resource limitation and adjust the intelligent splitting method, offering low energy in IoT applications. In addition, the authors in [17] studied the RA techniques for harvesting energy to establish an EE that considered sub-channel allocation, power control, and time allocation. The authors in [17] proposed reinforcement learning-based RA to improve the EE of an EH-enable IoT network supported by SWIPT. It is important to achieve low energy and improve the training efficiency and stability for every training epoch from the output layer to the hidden layer. Therefore, loss functions are computed for the weights of the hidden layer and updated by the optimizer of lower-order moments for the Adam algorithm through two gradient-based optimizations [22] and the stochastic gradient descent algorithm [23].

The chain rule is applied during the differentiation process. The procedure is carried out continuously until the loss function reaches a certain point [18], [24], [25], [26]. The authors in [24] studied the intelligent frequency, energy RA, and time RA for the EH-NOMA IoT systems to minimize the average number of packet losses for primary and secondary users. Due to the non-convexity of the optimization problem in [24], the authors proposed a deep deterministic policy gradient to improve the training efficiency and stability. This work was the first to investigate the DNN-based RA in MISO-SWIPT-IoT networks for EH. Therefore, we considered the MISO-SWIPT systems employed the PS approach to harvest energy for IoT devices to maximize EE. An advantage of DNN is that access to large labeled datasets is not required because labeling gets more complicated with increasing data volume. We chose the DNN technique to specify an exact weight and bias term in layers with extensive training to address non-channel interference and manage power control of transmitters to harvest energy with limited battery life. It depended on the SWIPT system to use EH to prolong the battery life of IoT devices based on finding an optimal solution for PA by applying the partial derivative of Lagrange Dual Decomposition (LDD) and Karush-Kuhn-Tucker (KKT) conditions. Updating the transmission power, PS ratio, and non-convex problems is time-consuming and does not ensure optimal achievement. Therefore, this work improved the network's life cycle and achieved the optimal RA to approximate the optimal PA. In addition, the ultra-low power devices harvesting energy in PS depended on avoiding training failure based on applying the chain's rules for DNNs training. This research proposed a novel training for DNN algorithms by applying Gradient Descent (GD) with chain rules to minimize the loss function based on updating the parameters of the weights hidden layer and convergence training to achieve near-optimal performance and minimize unneeded label data. The chain rule is applied during the differentiation process and prevents the training failure (fixed DNN) based on the weight in a hidden layer on the partial derivative of the input vectors. This work improved the network's life cycle and achieved the optimal RA to approximate the optimal PA, which depends on avoiding training failure based on applying the chain's rules for DNN training.

B. MOTIVATION AND CONTRIBUTIONS

The new approaches addressed the energy sustainability of IoT systems comprising increased EE with low EH. This research investigates how the transmit-harvest response in MISO-SWIPT-IoT systems is affected by co-channel interference. Transmission of data signals by transmitters, information decoding, EH by receivers via power splitting, and response to transmitters are all part of it. Enhancing IoT device transmission power and EE is the goal. Concerning power is convex power $\mathcal{P}_k$ and rate $\mathcal{R}_k$ is concave. The DNN was trained to compute the optimal approach with a smaller loss function and enable real-time updates for the association rule. Using an optimal iterative technique, we first create suboptimal solutions. We then present an effective framework for DNNs and a novel training approach that blends supervised and unsupervised training. By using the chain rule for the GD algorithm, this method seeks to avoid training failure. Through repeated weight updates in hidden layers, the GD algorithm finds the best weights for every neural network parameter. The network can determine whether weight adjustments are required to improve output accuracy and reduce loss by adjusting key neuron parameters through the use of the chain rule. The contributions of this paper are as follows:

- It proposes an EH for the taken-into-consideration MISO-SWIPT-IoT system to maximize the minimal harvested energy among IoT while meeting QoS requirements. Every IoT device was assumed to have PS that supported EH and maintained a QoS requirement. We studied the joint design of TX power needed to satisfy QoS and EH requirements. In addition, we investigated the optimization of TX

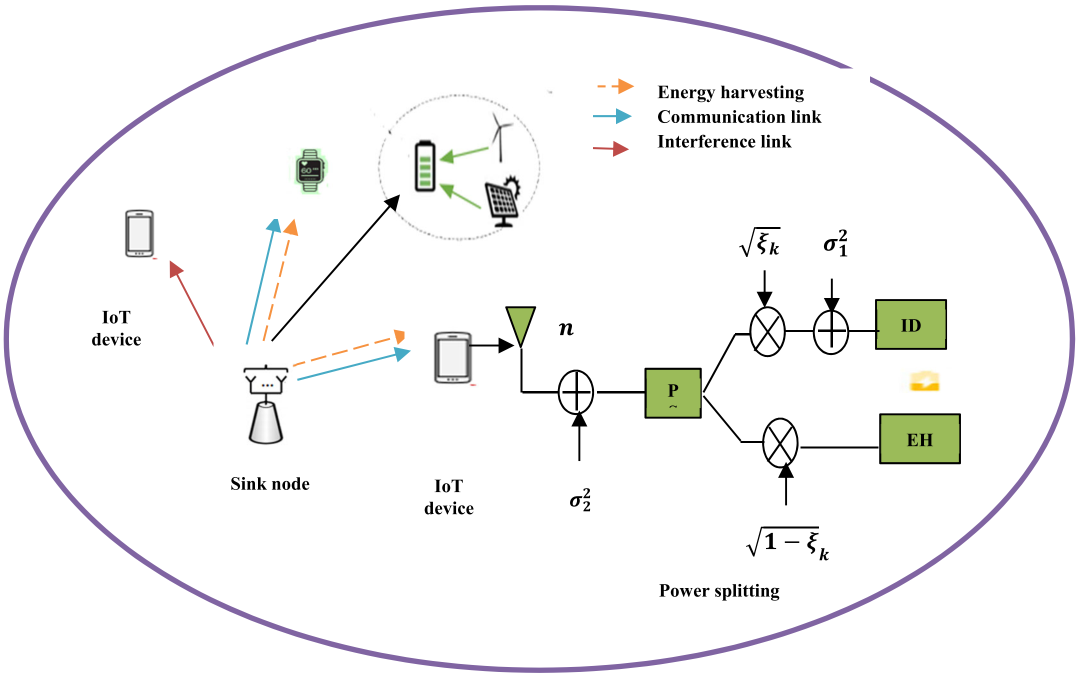

FIGURE 1. System model for SWIPT where the EH receivers are close to the sink node for EE reception.

precoding and PS ratio depending on whether RXs were needed to complete ID and EH.

• It provides new insight into the impact of the EH requirement on the RA efficiency for the interference channel. Existing approaches often rely on static rule-based optimization strategies, which may not adapt well to maximize the minimal harvested energy by providing new insight into the impact of the EH requirement on the RA efficiency for the interference channel. To address this limitation, the proposed algorithm jointly can explore the Optimize the Transmit Power and PS Ratios (OTPR) to RF EH ξ_k by improving the EE with ultra-low power devices EH in PS mode. It also minimizes the total energy consumption under the minimal harvested power $\mathbb{E}_{min}$ and optimal PS ratio from TX to $\mathrm{RX_k}$ for IoT devices.

• It ensures strong duality of the non-convex and Non-deterministic Polynomial (NP)-hard problems for the global optimizing power without loss gain for all $\mathrm{RX_k}$. We studied the EE optimization problem using the partial derivative of LDD and KKT conditions to optimize the channel allocation jointly, optimal PS ratio, and power control.

• Some existing approaches prioritize EE at the expense of model accuracy by resolving the increased time. To overcome this limitation, the DNNs are proposed to increase the output accuracy and reduce the loss in terms of optimal jointly optimizing PA $\mathcal{P}_k$ and IoT PS ratios to RF EH ξ_k regression against channel gains. Training DNN algorithms with chain rules often involves tuning a large number of hyperparameters, which can be time-consuming and computationally expensive. One potential strategy to address this limitation is by applying the GD of forward neural networks (FNN) to accelerate the learning process, and an estimate of the gradient in each iteration increases the accuracy of the output, reduces the loss, and reduces the complexity of the conventional iterative scheme.It was achieved by designing weight parameters to increase the learning rate and decrease the interference based on updated weight ω, and bias $\vec{b}$ of the DNN. The DNN for chain rule is proposed to adjust the weights to convergence training and achieve near-optimal performance by minimizing unneeded labeled data to avoid failure training.

• From extensive simulations of the performance comparisons of the DNN with the OTPR under various system parameters, the DNN algorithms chain rules provided a near-optimal performance EE with less computation time than the OTPR. In particular, it is demonstrated that the proposed DNN achieves performances comparable to those of an Exhaustive Search (ES) but with the shortest training time.

II. SYSTEM MODEL

This study presents the IoT system using a MISO SWIPT with the adopted channel as shown. A multi-antenna TX was responsible for transmitting information and power to low-power and data-hungry EH PS RXs. The IoT system under consideration consisted of K single-antenna IoTs denoted by $\mathrm{RX_k}$ $\forall k \in \mathbb{K} = [1, 2, \ldots, \mathrm{K}]$, and the sink node was called the TX. Every Rx was considered wireless-powered to guarantee the individual minimum EH in K-link interference channels, allow the harvest of a particular amount of energy, and improve RF-received signal transport for the IoT device by using the PS technique as shown in

Fig. 1 [27]. The channel between N-antenna TX and the single-antenna RX_k was denoted as $\mathfrak{h}_k \in \mathbb{C}^{N\times 1}$ $\forall k \in \mathbb{K}$. It was necessary to secure the line of sight to harvest enough energy from the RF signals; therefore, the channel power gain, $|\mathfrak{h}_k|^2$, was an independent identically-distributed Rician random variable with a mean of $\mathcal{E}_k$. Moreover, the noise in the RF signal and the noise power of an antenna in an EH receiver depended on the ambient environment and the antenna's loss resistance. The RX_k could not harvest energy from these noises because the far-field RF power was insufficient to achieve the sensitivity level required for RF EH [28]. The baseband and antenna noise powers at the IoT device were denoted by n_1^2 and n_2^2, represented as $n_1^2 \sim \mathcal{CN}\left(0, \sigma_1^2\right)$ and $n_2^2 \sim \mathcal{CN}\left(0, \sigma_2^2\right)$, respectively. It was assumed that the IoT device was equipped with a PS policy to exploit the SWIPT function. The channel gain was constant during one coherence interval and varied independently in subsequent intervals [29], [30], [31]. The received RF signal $\mathcal{Y}_k \in \mathbb{C}$ of RX_k, can be written as:

$$\mathcal{Y}_k = \mathfrak{h}_k \mathcal{Z}_k + \sum\nolimits_{j\in\mathbb{K}\setminus\{k\}} \mathfrak{h}_j \mathcal{Z}_j + n, \tag{1}$$

where $\mathcal{Z}_k \in \mathbb{C} \forall k \in \mathbb{K}$ represents the data symbol transmitted by TX and intended for RX_k, and n represents RF signal noise referring to complex additive white Gaussian noise with variance σ_n^2. The PS scheme [28], [32] allowed the network to split and utilize the RF EH for the RX_k RF signals at a time shown in (1). When a PS RX_k operated in the EH mode, the EH from TX was written as $\mathbb{E}_k = \vartheta \mathcal{P}_k |\mathfrak{h}_k|^2$. The ϑ and $\mathcal{P}_k$ denote the EH efficiency factor used at every K RXs and the transmit power of the TX, respectively. The channel power gain was modeled as $\psi_k = |\mathfrak{h}_k|^2 d_k^{-\alpha}$, where d and α represent a long-distance transmission between TX and RX_k for data and the path loss exponent, respectively. When the time switching received RX_k working in the information decoding mode, the maximum rate from TX was $r_k = \mathbb{W}\log_2\left(1 + \mathcal{P}_k |\mathfrak{h}_k|^2/\sigma_1^2\right)$. The $\mathbb{W}$ is the transmission bandwidth. However, the received signal for every RX_k divided the time for receiving signals from TX in the PS into two streams: (i) the RF signals to the EH with different power levels as $\xi_k \in [0, 1]$ for $k \in \mathbb{K}$, and (ii) the slot's remaining time used for transmitting the information data decoding $(1 - \xi_k)$.

$$\mathbb{E}_k = \vartheta(1 - \xi_k) \sum\nolimits_{j\in\mathbb{K}\setminus\{k\}} \mathcal{P}_k \psi_k. \tag{2}$$

The QoS of the received RF for the information data decoding receiver, $\mathcal{R}_k$, is given by

$$\begin{aligned} \mathcal{R}_k &= \mathbb{W}\log_2\left(1 + \frac{\xi_k \mathcal{P}_k |\mathfrak{h}_k|^2}{\sigma_1^2 + \sigma_2^2}\right) \\ &= \mathbb{W}\log_2\left(1 + \frac{\xi_k}{\sigma_1^2 + \sigma_2^2} \sum\nolimits_{j\in\mathbb{K}\setminus\{k\}} \mathcal{P}_k \psi_k\right). \end{aligned} \tag{3}$$

The data rate of the Tx must fulfill $\mathcal{R}_k^{Tx} > \mathcal{R}_1$ to satisfy QoS requirements for a TX, where $\mathcal{R}_1$ represents the rate threshold of each TX. In addition, to decode RX_k successfully, the information rate of RX_k must meet $\mathcal{R}_k^{Rx} > \mathcal{R}_2$, where $\mathcal{R}_0$ represents the threshold rates for all RX_k. Every RX_k was considered wirelessly powered and required harvesting a particular amount of energy from the RX_k signal using a PS. The PS accomplished superior trade-offs between the information rate and the amount of RF energy conveyed.

III. PROBLEM FORMULATION

This study aimed to maximize the EE ultra-low power devices EH in PS mode by determining a combined EH to IoT device and optimal PS ratio from TX to RX_k. The power consumption P_{conv} in conventional wireless communication can be written as:

$$P_{conv} = \gamma \sum\nolimits_{j\in\mathbb{K}\setminus\{k\}} \mathcal{P}_k + P_c, \tag{4}$$

where γ and P_c are the power amplifier drain efficiency and circuit power consumption at the EH, respectively. Utilizing the PA optimization problem guarantees minimum EH requirements at RX_k and ultimate allowable transmit power at TX. The application utility functions can guarantee optimum performance from TX to RX_k that outperform conventional schedulers. The total RF power for each RX_k that can be used by an EH-enable IoT network supported by SWIPT is as follows:

$$P_{total} = \gamma \sum\nolimits_{j\in\mathbb{K}\setminus\{k\}} \mathcal{P}_k + P_c - \vartheta(1 - \xi_k) \sum\nolimits_{j\in\mathbb{K}\setminus\{k\}} \mathcal{P}_k \psi_k. \tag{5}$$

The joint design of TX precoding and IoT PS ratios for SWIPT networks improves by jointly optimizing PA $\mathcal{P}_k$ and IoT PS ratios to RF EH ξ_k to maximize EE. The problem is quasi-concave for $\mathcal{P}_k$ and ξ_k in massive connectivity for EE optimization criterion:

$$\Xi = \frac{\mathbb{W}\log_2\left(1 + \frac{\xi_k}{\sigma_1^2+\sigma_2^2} \sum_{j\in\mathbb{K}\setminus\{k\}} \mathcal{P}_k \psi_k\right)}{\gamma \sum_{j\in\mathbb{K}\setminus\{k\}} \mathcal{P}_k + P_c - \vartheta(1 - \xi_k) \sum_{j\in\mathbb{K}\setminus\{k\}} \mathcal{P}_k \psi_k}. \tag{6}$$

The goal was to maximize the EE (6) in non-convex and decreasing functions for RF signals to the EH with different power levels ξ_k. Concerning $\mathcal{P}_k$ and ξ_k, we compute the second-order condition of the total power of (5) and the information transmission rate of (3). P_{total} is convex with respect to $\mathcal{P}_k$ and $\mathcal{R}_k$ is concave, as shown by equations (7) and (8). The efficient conventional successive convex function in (6) was obtained using the second-order derivatives of $\mathcal{P}_k$ and ξ_k [29], [33]:

$$\frac{\partial^2 \mathcal{R}_k}{\partial^2 \mathcal{P}_k} = -\frac{\mathbb{W}\xi_k^2 \sum_{j\in\mathbb{K}\setminus\{k\}} \psi_k^2}{\ln 2 * \left(\sigma_1^2 + \sigma_2^2 + \xi_k \sum_{j\in\mathbb{K}\setminus\{k\}} \mathcal{P}_k \psi_k\right)^2} < 0\,, \tag{7}$$

$$\frac{\partial^2 \mathcal{R}_k}{\partial^2 \xi_k} = -\frac{\mathbb{W} \sum_{j\in\mathbb{K}\setminus\{k\}} \mathcal{P}_k^2 \psi_k^2}{\ln 2 * \left(\sigma_1^2 + \sigma_2^2 + \xi_k \sum_{j\in\mathbb{K}\setminus\{k\}} \mathcal{P}_k \psi_k\right)^2} < 0\,. \tag{8}$$

From (7) and (8), the EH is an affine function that is positive in the denominator with $\mathcal{P}_k$. Consequently, the EE is a quasi-concave function. Our goal was to minimize the total energy consumption by maximizing the minimum harvested power $\mathbb{E}_{min}$. The problem of EE maximization can be written as follows:

$$\max_{0\leq\mathcal{P}_k, 0\leq\xi_k\leq 1} \quad \Xi\,, \tag{9}$$

$$\text{s.t.} \ \mathbb{E}_k(\mathcal{P}_k,\ \xi_k) > \ \mathbb{E}_{min}, \tag{9a}$$

$$0 < \mathcal{P}_k \leq \mathrm{p}_k^{max}, \tag{9b}$$

$$\mathcal{P}_k \geq 0, \tag{9c}$$

$$0 < \xi_k < 1, \tag{9d}$$

where $\mathbb{E}_{min}$ and p_k^{max} represent the EH requirement at RX_k and the maximum allowable transmit power at Tx, respectively. Constraint $\mathbb{E}_{min}$ in (9a) should meet the minimum EH requirement. The constraint in (9b) represents the maximal available power, which limits the transmit power and PS ratios to the Tx and RX_k, respectively. The constraint in (9c) represents the ranges of wireless transmission power. The problem in (9d) sets the range of the PS constraint ξ_k between 0 and 1.

IV. PROBLEM SOLUTION

A. OPTIMAL ITERATIVE ALGORITHM

Given that the optimization problem (9) is non-convex because of the co-channel interference and NP-hardness [34], optimizing power and good channel without loss gain for all RX_k are proposed based on applying a joint conventional OTPR algorithm solution to maximize EE. The EE subject to constraints (9)–(9d) is difficult to derive, so the Lagrange function of problem (9)–(9d), can be written as

$$\mathcal{L}\left(\mathcal{P}_k,\ \xi_k, \mu,\ \nu, \lambda, \delta\ \right) = \frac{\mathrm{W}\log_2\left(1+\frac{\xi_k}{\sigma_1^2+\sigma_2^2}\sum_{j\in\mathbb{K}\backslash\{k\}}\mathcal{P}_k\psi_k\right)}{\gamma\sum_{j\in\mathbb{K}\backslash\{k\}}\mathcal{P}_k+P_c-\vartheta(1-\xi_k)\ \sum_{j\in\mathbb{K}\backslash\{k\}}\mathcal{P}_k\psi_k} + \mu_k\left(\mathbb{E}_k-\mathbb{E}_{min}\right)+\sum\nolimits_{j\in\mathbb{K}\backslash\{k\}}\nu_k\left(\mathrm{p}_k^{max}-\mathcal{P}_k\right) + \sum\nolimits_{j\in\mathbb{K}\backslash\{k\}}\lambda_k\mathcal{P}_k+\delta_k\left(1-\xi_k\right), \tag{10}$$

where $\mu,\ \nu, \lambda, \delta$ are the Lagrangian multipliers related to constraints for (9)–(9d), respectively. The EE obtained by partial derivative of LDD and KKT conditions to obtain the global solution of (9)–(9d) for the EE maximization problem given in (10). To simplest the equation we suppose $\mathcal{J} = \ \ln 2 * \left(\sigma_1^2+\sigma_2^2+\xi_k^*\sum_{j\in\mathbb{K}\backslash\{k\}}\mathcal{P}_k^*\psi_k\right) \left(\gamma\sum_{j\in\mathbb{K}\backslash\{k\}}\mathcal{P}_k^*+P_c-\vartheta(1-\xi_k^*)\ \sum_{j\in\mathbb{K}\backslash\{k\}}\mathcal{P}_k^*\psi_k\right)$, and $\varsigma = \left(\gamma\sum_{j\in\mathbb{K}\backslash\{k\}}\mathcal{P}_k^*+P_c-\vartheta\left(1-\xi_k^*\right)\sum_{j\in\mathbb{K}\backslash\{k\}}\mathcal{P}_k^*\psi_k\right)$. The optimal $\mathcal{P}_k$ and ξ_k can be derived by solving $\frac{\partial\mathcal{L}}{\partial\mathcal{P}_k}=0$ as in (11)–(14), shown at the bottom of the page.

From the quadratic formula, EE is a nonlinear problem, so we assign a partial derivative equal to zero from (11) and (12) to get the optimal power as shown at the bottom and upper of the page. The optimal values for KKT conditions $\mathcal{P}_k^*, \xi_k^*,\ \mu_k^*,\ \nu_k^*,\ \lambda_k^*,\ \delta_k^*$, must meet the following equations for all values of k:

$$\frac{\partial\mathcal{L}}{\partial\mathcal{P}_k} = \mathfrak{t}_k-\nu_k^*+\lambda_k^*, \tag{15}$$

$$\frac{\partial\mathcal{L}}{\partial\xi_k} = \mathfrak{T}_k-\mu_k^*\vartheta\sum\nolimits_{j\in\mathbb{K}\backslash\{k\}}\mathcal{P}_k^*\psi_k-\delta_k^*, \tag{16}$$

$$\mu_k^*\left(\mathbb{E}_k-\mathbb{E}_{min}\right)=0, \tag{17}$$

$$\nu_k^*\left(\mathrm{p}_k^{max}-\mathcal{P}_k\right)=0, \tag{18}$$

$$\lambda_k^*\mathcal{P}_k^*=0, \tag{19}$$

$$\delta_k^*\left(1-\xi_k^*\right)=0, \tag{20}$$

$$\mu_k^*,\ \nu_k^*,\ \lambda_k^*,\ \delta_k^*\geq 0. \tag{21}$$

From (15)–(21), the transmit power and EH should satisfy KKT conditions for the balancing looseness, $\lambda_k^* \neq 0$ if $\mathcal{P}_k^* \neq \mathrm{p}_k^{max}$. For the non-convex problem and guaranteed strong duality, the optimizing power without loss gain for all RX_k can be observed as $\psi_1 > \psi_2 > \ldots > \psi_k$. Due to the different channel gains ψ_k for all RX_k, the $\mathfrak{t}_k$ from (13)

$$\frac{\partial\mathcal{L}}{\partial\mathcal{P}_k} = \frac{\xi_k^*\psi_k}{\mathcal{J}} - \frac{\log_2\left(1+\frac{\xi_k^*}{\sigma_1^2+\sigma_2^2}\sum_{j\in\mathbb{K}\backslash\{k\}}\mathcal{P}_k^*\psi_k\right)\left(\gamma-\vartheta\left(1-\xi_k^*\right)\sum_{j\in\mathbb{K}\backslash\{k\}}\psi_k\right)}{\varsigma^2} + \vartheta\psi_k\left(1-\xi_k^*\right)\mu_k^*-\nu_k^*+\lambda_k^*, \tag{11}$$

$$\frac{\partial\mathcal{L}}{\partial\xi_k} = \frac{1}{\mathcal{J}} + \frac{\vartheta\log_2\left(1+\frac{\xi_k}{\sigma_1^2+\sigma_2^2}\sum_{j\in\mathbb{K}\backslash\{k\}}\mathcal{P}_k^*\psi_k\right)}{\varsigma^2}\times\sum\nolimits_{j\in\mathbb{K}\backslash\{k\}}\mathcal{P}_k^*\psi_k-\ \vartheta\mu_k^*-\sum\nolimits_{j\in\mathbb{K}\backslash\{k\}}\mathcal{P}_k^*\psi_k-\delta_k^*, \tag{12}$$

$$\mathfrak{t}_k = \frac{\xi_k^*\psi_k}{\mathcal{J}} - \frac{\log_2\left(1+\frac{\xi_k^*}{\sigma_1^2+\sigma_2^2}\sum_{j\in\mathbb{K}\backslash\{k\}}\mathcal{P}_k^*\psi_k\right)\left(\gamma-\vartheta\left(1-\xi_k^*\right)\sum_{j\in\mathbb{K}\backslash\{k\}}\psi_k\right)}{\varsigma^2} + \ \mu_k^*\vartheta\left(1-\xi_k^*\right)\psi_k, \tag{13}$$

$$\mathfrak{T}_k = \left[\frac{1}{\mathcal{J}} + \frac{\vartheta\log_2\left(1+\frac{\xi_k}{\sigma_1^2+\sigma_2^2}\sum_{j\in\mathbb{K}\backslash\{k\}}\mathcal{P}_k^*\psi_k\right)}{\varsigma^2}\right]\sum\nolimits_{j\in\mathbb{K}\backslash\{k\}}\mathcal{P}_k^*\psi_k. \tag{14}$$

changes with respect to ψ_k. The IoT device must also detect how the channels' properties differ over time and space to select a good channel. If $t_k < 0$, the multiplier $\lambda_k^* > 0$, and the optimal solution can be obtained as $\mathcal{P}_k^* = 0$ according to the looseness (19). However, if $t_k > 0$, the optimal solution can be obtained when $\mathcal{P}_k^* \neq p_k^{max}$, according to (18) and (21). For $t_k = 0$, the optimal $\mathcal{P}_k^*$ TX precoding for information data decoding (i.e., no EH) can be obtained as $(p_k^{max} - \mathcal{P}_k)$ and $\nu_k^* = \lambda_k^* = 0$ according to looseness in (15). The optimal PA for all RX_k can be expressed as $\mathcal{P}_k = \{p_1^{max},\ p_2^{max},\ \ldots,\ p_{k-1}^{max},\ \mathcal{Z}_k^*,\ 0, \ldots, 0\ ,\ 0\}$. The EE is maximized by the obtaining optimal PA, given as $\mathcal{P}_k^* = \min\left(\max\left(0,\ \mathcal{Z}_k^*\right), p_k^{max}\right)$ with a feasible region $\{0\ , \mathcal{Z}_k^*\}$. The EE increases as the PS ratio rises, the least EH is determined from the constraint (17), and the best PS ratio is given as

$$\xi_k^* = 1 - \frac{\mathbb{E}_{min}}{\vartheta \sum_{j\in\mathbb{K}\setminus\{k\}} \mathcal{P}_k^* \psi_k}. \tag{22}$$

Using the best PA $\mathcal{P}_k^*$, the EE maximization problem can be solved by applying the Lambert function-based closed-form to achieve near-optimal EE in (24).

$$\Xi = \frac{\ln\left(\frac{\mathcal{P}_k^* \psi_k}{(\sigma_1^2+\sigma_2^2)} + q_k\right)}{\mathcal{P}_k^* + P_c - \mathbb{E}_{min}}, \tag{23}$$

where

$$q_k = 1 - \frac{\mathbb{E}_{min}}{\vartheta\left(\sigma_1^2+\sigma_2^2\right)} + \frac{\sum_{j\in\mathbb{K}\setminus\{k\}} \mathcal{P}_k^{max} \psi_k}{\left(\sigma_1^2+\sigma_2^2\right)}.$$

$$\mathcal{Z}_k^* = \frac{\left(\sigma_1^2+\sigma_2^2\right)}{\psi_k} e^{\left(\omega\left(\frac{\frac{\psi_k(P_c-\mathbb{E}_{min}-q_k)}{(\sigma_1^2+\sigma_2^2)}}{e}\right)+1\right)-q_k}$$
$$\text{if} \frac{\psi_k}{\left(\sigma_1^2+\sigma_2^2\right)}\left(P_c - \mathbb{E}_{min}\right) - q_k \geq -1\ , \tag{24}$$

where ω and e^{ω} represent the complex number and the exponential function [35]. The ω is the multivalued function, the inverse of $(f\ (\omega) = \omega e^{\omega})$. It should be noted that the long computation time increases exponentially with N and K, and the complexity becomes $\mathcal{O}(N^{2\mathrm{K}})$ [36]. The proposed algorithm for the Lagrangian multiplier method and KKT conditions assumed that the $\mathcal{P}_k$ and EH are executed individually at different times to guarantee convergence of the Lambert function to achieve a near-optimal EE. Therefore, the transmit power $\mathcal{P}_k = 0$ when the time slot for $k \in \mathbb{K}$ is allocated to EH. With the computational enabled by the proposed algorithm, a sufficiently small step size is required to update each transmit power and EH ratio. However, this update for transmitting power and EH ratio increases the required time considerably. Therefore, the proposed algorithm's solutions do not guarantee optimal achievement, and non-convex problems are challenging. As a naive method for obtaining the optimal solution, we consider an ES to find the best solution for high training time. Many iterative strategies, including the genetic algorithm and simulated annealing, are available in the literature to find the best non-convex programming solution in addition to the ES approach. However, algorithm I take long to converge, making them unsuitable for real-time processing networks. to overcome these difficulties the neural networks training reduced the complexity of the conventional iterative scheme, as shown in the following section.

Algorithm 1 OTPR Algorithm for Updating a Transmit Power and Maximization EE

1. **Input:** Channel power gain as $\psi_1 > \psi_2 > \ldots. > \psi_k,\ \mathcal{P}_k,\ \xi_k,\ \Xi = 0$.
2. **Output:** $\mathcal{P}_k^*, \xi_k^*\ ,\ \ \forall k$;
3. Solve the optimization problem in (9) to obtain $\mathcal{P}_{k,}$ and $\xi_k\ \ \forall k$, to get the $\mathcal{P}_k^*$, and ξ_k^*;
4. **While**$(k < \mathrm{K})$
5. $k = k + 1$
6. Compute t_k, and T_k
7. **If** $(\mathcal{P}_k^* = p_k^{max})$ then
8. **Update** the Lagrangian multiplier method and KKT conditions by (15)-(21), and $\mathcal{P}_k^* = \min\left(\max\left(0,\ \mathcal{Z}_k^*\right), p_k^{max}\right)$
9. **Else**
10. **Set** $\mathcal{P}_k^* = 0$
11. **End if**
12. **End while**
13. **Compute** the PS ratio ξ_k^* according (22) and obtain near-optimal EE.

B. NEURAL NETWORKS-BASED DEEP LEARNING

DNN-based learning in RA aims to maximize the efficiency of the B5G system. In this article, improving the network life cycle and achieving the optimal RA for approximating the optimal value of $\mathcal{P}_k$ and ξ_k depended on solving the optimization problem (9). It was important to create appropriate models for using neural network training for quick and accurate RA in terms of the regression of optimal $\mathcal{P}_k$ and ξ_k against channel gains. The input vector was specified as $\vec{\mathfrak{z}} \in \mathbb{R}^{\mathrm{K}^2\times 1}$ given to the network through the input layer K^2.

$$\mathfrak{z}_{\mathrm{K}(k-1)} = \left|\mathfrak{h}_k\right|^2, \quad \forall\, k \in \mathbb{K}. \tag{25}$$

The emphasis was on FNNs with fully connected layers for RA. The input layer contained K^2 neurons that passed information to the hidden layer $(\mathcal{L})$, which had N_l neurons as shown in Fig. 2. The number of hidden layers $\mathcal{L} = 4$ with $\mathrm{N}_l = 96$ neurons in every hidden layer. The output layers $(\mathrm{N}_{\mathcal{L}}+1)$ neurons extracted the $(\mathrm{N}_{\mathcal{L}}+1)-$dimensional output. Let $\mathcal{X}_{l-1}$ represent the input to the $l-th$ layer of the network as $\mathfrak{z}_{l-1}$. The output $\mathcal{X}_l(\varkappa)$ of neuron $\varkappa$ in layer l was determined as $l = 1, \ldots,\ \mathcal{L}+1$ and $\varkappa = 1, \ldots, \mathrm{N}_l$:

$$\mathcal{X}_l\ (\varkappa) = \int_{\varkappa,l} \left(\mathfrak{z}_{\varkappa,l}\right), \quad \mathfrak{z}_{\varkappa,l} = \omega_{\varkappa,l}\mathcal{X}_{l-1} + \mathfrak{b}_{\varkappa,l}, \tag{26}$$

where $\omega_{\varkappa,l} \in \mathbb{R}^{\mathrm{N}_{l-1}}$ and $\mathfrak{b}_{\varkappa,l} \in \mathbb{R}$ are the weight matrix and bias term in layer l, respectively. The final output was

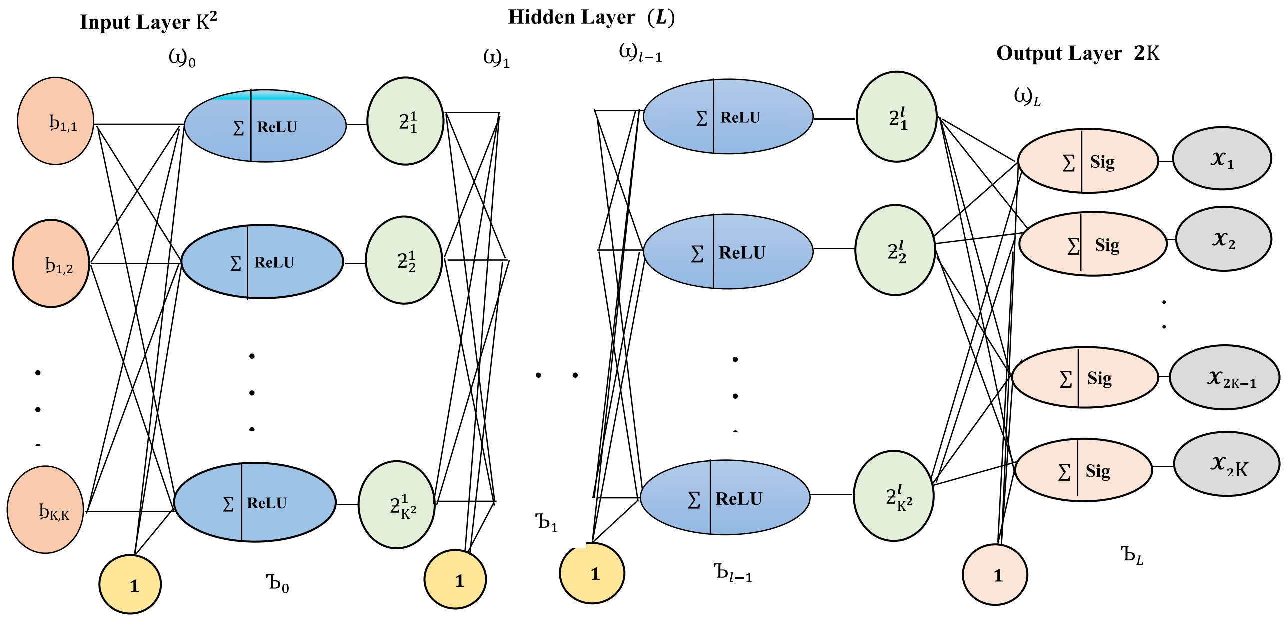

FIGURE 2. Scheme of feedforward DNN with fully connected layers.

obtained by applying the activation function $f_{\text{и},l}$ to $z_{\text{и},l}$ in the hidden layers using the rectified linear unit ReLU $(z_{\text{и},l}) = \max(0,\ z_{\text{и},l})$, which denotes a sigmoid function as:

$$\sigma(z_{\text{и},l}) = \frac{1}{1+e^{-z_{\text{и},l}}}. \tag{27}$$

The sigmoid function is employed as the gate control mechanism in a particular kind of Recurrent Neural Network (RNN) to manage information flow. To be more precise, the input gate, forget gate, and output gate of units use the sigmoid function to determine which data to accept and which to reject.

C. TRAINING NEURAL NETWORKS

This study adjusted the parameters $\omega_{\text{и},l}$ and $\text{Ъ}_{\text{и},l}$ by training a neural network for the regression of optimal values of $\mathcal{P}_k$ and ξ_k against channel gains for the FNN to learn the desired input-output relation. Based on the forwarded node values of the final output of the hidden layer, the Resource Control (RC) vector ($\vec{\mathcal{X}} \in \mathbb{R}^{2\mathrm{K}\times 1}$ was processed at 2K nodes of the output layer [37], [38]. For every layer $l = 1, \ldots, \mathcal{L}+1$, let the weight vectors $\omega_l = [w_{1,l},\ \ldots,\ w_{\mathrm{N}_{l,l}}] \in \mathbb{R}^{\mathrm{N}_{l-1}\times \mathrm{N}_l}$ and bias into vector $\text{Ъ}_l = [b_{1,l},\ \ldots,\ b_{\mathrm{N}_{l,l}}]^T \in \mathbb{R}^{\mathrm{N}_l\times 1}$, where $[b_{1,l},\ \ldots,\ b_{\mathrm{N}_{l,l}}]^T$ means Ъ_l transpose as:

$$(\vec{\mathcal{X}} = \sigma(\omega_{\text{и},\mathcal{L}+1}\mathcal{X}_{\mathcal{L}}\ (\text{и}) + \text{Ъ}_{\text{и},\mathcal{L}+1}). \tag{28}$$

With this output vector $\vec{\mathcal{X}}$, $\vec{\mathcal{P}}_k$ and $\vec{\xi}_k$ were defined as:

$$\mathcal{P}_k = \mathrm{p}^{\max}\mathcal{X}_{K+k}\ ,\quad \xi_k = \mathcal{X}_k \quad \textit{for } k \in [1, \ldots\ldots, \mathrm{K}]. \tag{29}$$

The neuron output in (26) can characterize more complicated connections between the channel state and the optimal RC vector as $\mathcal{L}+1$ when N_l increases. In addition, the training data in (26) aimed to minimize the loss between the channel condition and the optimal RC vector by optimizing the network ω_l and Ъ_l for all training.

A novel training strategy that combines supervised and unsupervised techniques to construct an efficient DNN framework is proposed to improve the performance evaluation and decrease the computing time in the RF-EH IoT system. Using iterative algorithm solutions, the DNN model is first supervised and trained in this manner to approximate the performance of the optimal iterative algorithm. The optimization problem in (9) was directly applied to the loss function. Recent advancements in $\mathcal{P}_k$ regulation based on NN [22], [23], [39], where the loss is directly derived from EE, follow $\text{Ł}(\omega, \text{Ъ}) = -\Xi(\mathrm{p}^{\max}\mathcal{X}_{[1:\mathrm{K}]},\ \mathcal{X}_{[\mathrm{K}+1:2\mathrm{K}]})$. To improve EE, we created a new loss function:

$$\text{Ł}(\omega, \text{Ъ}) = \frac{\sum_{\mathrm{k}\in\mathbb{K}} \ w_{\mathrm{k}}\mathcal{R}_{\mathrm{k}}(\mathrm{p}^{\max}\vec{\mathcal{X}}_{[1:\mathrm{K}]},\ \vec{\mathcal{X}}_{[\mathrm{K}+1:2\ \mathrm{K}]})}{\mathrm{p}^{\max}\vec{\mathcal{X}}_{[1:\mathrm{K}]},\ \vec{\mathcal{X}}_{[\mathrm{K}+1:2\ \mathrm{K}]}}, \tag{30}$$

where $w_k = \frac{\left|\text{ђ}_k\right|^2 d_k^{-\alpha}}{\sum_{j\in\mathbb{K}\setminus\{k\}}\left|\text{ђ}_k\right|^2 d_k^{-\alpha}} / \frac{\psi_k}{\sum_{j\in\mathbb{K}\setminus\{k\}}\psi_k}$ represents the weight parameter. Since the loss function $\text{Ł}(\omega, \text{Ъ})$ does not perform well in interference, we utilized the weight parameter w_k to the rate $\mathcal{R}_k$ in the loss function to enhance learning in interference-limited situations. Compared to a normal loss function without w_k, including w_k in the loss function improved learning performance under interference-limited circumstances. From (30), the weight parameter w_k was designed to increase the learning rate with decreasing interference based on updated ω and $(\vec{\text{Ъ}})$ of the

DNN. The primary motivation was to utilize the supervised learning's fast convergence training speed to minimize unneeded label data from unsupervised learning. The $\mathcal{P}^*_{k,PS}$ and IoT PS ratiosto RF EH ξ^*_k were used as labeled data to pre-train DNN and replicate an optimization-based RA strategy. To reduce the need for labeled data in unsupervised learning, the DNN model then takes advantage of the quick training convergence of supervised learning. Without depending on labeled data to determine the best resource management plan, a carefully constructed loss function is created to directly approximate the ideal transmit power and EH ratio from training channel samples. During the training, the loss function was taken into consideration PS. The mean square error enabled a simple computation that continuously adjusted the weights to convergence training and achieved near-optimal performance by minimizing unneeded label data as $\sum_{k\in\mathbb{K}} \left\|(\mathcal{P}^*_k - \mathcal{P}_k) + (\xi^*_k - \xi_k)\right\|^2$ [10], [40]. An estimate of (30) was computed as the true gradient using a randomly selected subset of the entire training data set to reduce the loss function with each iteration of the gradients. The GD continuously updated the parameters for each $(Ѡ, Ъ)$ to minimize the loss function for FNN set as:

$$Ѡ_{new} = Ѡ_{old} - \delta \frac{\partial Ł(Ѡ, Ъ)}{\partial Ѡ}, \tag{31}$$

$$Ъ_{new} = Ъ_{old} - \delta \frac{\partial Ł(Ѡ, Ъ)}{\partial Ъ}, \tag{32}$$

where δ represents a learning rate that determines how quickly $Ѡ$ and $Ъ$ change. The gradients of each node in (26) determined if each node's updated weights had changed. Every time the gradient of each node was calculated, the estimated gradient (30) was evaluated by updating a new randomly selected weightfrom (31). Then, (32) was used to obtain optimal $\mathcal{P}^*_k$ and IoT PS ratiosto RF EH ξ^*_k in place of the true gradient.The partial derivative in the second terms of (31) and (32) reached a maximum value, which decreased until the partial derivative of the loss function had a value close to zero. The GD depended on a weight initialization by assigning initial values to the weights in the neural network. The deep learning approach faced difficulty in learning efficient RA because of the EH requirements for TX-RX. It occurred due to treating an unprocessed channel gain in the DNN entries, leading to training failure created from the highly variable channel gains with various path losses (25). To avoid the origins of training failures, we applied a chain rule for GD, shown in the following section.

D. AVOIDING THE TRAINING FAILURE BASED ON THE CHAIN RULE FOR THE GD ALGORITHM FOR FNN TRAINING

The proposed GD for FNN was used to accelerate the learning process and estimate the gradient in each iteration [24], [25], [26] to preventtraining failure and circumvent the zero gradient $Ł(Ѡ_{old}, Ъ_{old}) = 0$ problems (31). The loss function gradient was represented using the chain rule of partial derivatives as the product of the gradients of activation functions $f_{и,l}$ to $Ƶ_{и,l}$ in the hidden layersin (27) for $Ѡ$ and $Ъ$. However, the loss function (31) was terminated due to training failure in other environments caused by the difficulty of updating the parameters with zero gradient $Ł(Ѡ_{old}, Ъ_{old}) = 0$ when any EH constraints were violated. By applying the chain rule for the error gradient of the loss function that considered all network weights, the training failure was avoided as it used the partial derivative of neuron, $Ƶ_{и,l}$ with respect to $Ƶ$ and neuron $N_l(Ƶ) = \max(0, Ƶ) = \max(0, sum(Ѡ \otimes \mathcal{X}_{l-1} + Ъ)$, which treated negative values as zero. The GD algorithm operated based on the true gradient estimate for all values of $Ƶ$ less than or greater than zero and obtained the derivative as:

$$\frac{\partial}{\partial Ƶ_k}\max(0, Ƶ) = \begin{cases} 0 & Ƶ \le 0 \\ \frac{\partial Ƶ_k}{\partial Ƶ_k} = 1 & Ƶ > 0. \end{cases} \tag{33}$$

The applied chain rule $\partial N_l / \partial Ѡ$ determined the derivative of the inner part of the composite function in the layer l as $l = 1, \ldots, \mathcal{L}+1$ and $и = 1, \ldots, N_l$. After computing the loss function for each weight, the GD determined the optimal weights for all neural network weights depending on updating the parameters of the weights hidden layer and convergence training to achieve near-optimal performance and minimize unneeded label data. The chain rule adjusted the $Ѡ_{old}$ and the $Ъ_{old}$ within certain neurons and enabled the network to identify whether that weight needed to be increased or decreased to improve the output accuracy and reduce the loss. The multiplier obtained the derivative of neurons for both parts in terms of $Ѡ$:

$$\frac{\partial N_l}{\partial Ѡ} = \frac{\partial N_l}{\partial Ƶ_k}\frac{\partial Ƶ_k}{\partial Ѡ} = \begin{cases} \frac{\partial Ƶ_k}{\partial Ѡ} = 0^T & Ƶ \le 0 \\ \frac{\partial Ƶ_k}{\partial Ѡ} = (\mathcal{X}_L(и))^T & Ƶ > 0. \end{cases} \tag{34}$$

The EH constraints were rarely violated based on a good training performance in (30) settings where the available p^{max} was high. Since the $Ѡ_{old}$ and new values remained the same, the node was treated as dead under such circumstances. A leaky ReLU kept the GD from dropping to zero, and its usage depended on overcoming the training failure from treating unprocessed channels (25). The DNN model needed to be retrained whenever any training parameter was altered because all parameters, such as $\mathcal{R}_k$ and p^{max}, were fixed during training due to the weight, w_k, lost to the rate, $\mathcal{R}_k$. To compute the gradients using a chain rule in (26), we defined the input vector $Ƶ_k$ as:

$$Ƶ_k = \begin{cases} \frac{(K^2 Ƶ_k - \sum_{k\in\nu} Ƶ_k)}{\sum_{k\in K} Ƶ_k} & k \in \{1, \ldots, K\} \\ p^{max}\frac{1}{K^2}\sum_{k\in\mathbb{K}} Ƶ_k & k \in \{1, \ldots, K\}. \end{cases} \tag{35}$$

Utilizing the chain rule for the GD algorithm for FNN pre-training in conjunction with (35) yields the transmit power and EH. The main driving force behind this was to reduce the amount of unnecessary label data from unsupervised learning by making use of supervised learning's quick training convergence. The labeled data used for pre-training DNN and replicating an optimization-based RA method was the $\mathcal{P}^*_{k,PS}$ and IoT PS ratios to RF EH ξ^*_k. In light of considering unprocessed channels as a means of overcoming training failure (25). The training was updated by the applied chain rule in (34) by enhancing learning stability, speed, and efficiency by determining the weight in a hidden layer on the partial derivative of the input vectors. The applied chain rule updated the training and prevented the training failure (fixed DNN) based on the weight in a hidden layer on the partial derivative of the input vectors in (34). It was achieved by increasing learning stability, speed, and efficiency by finding the best training strategy. The efficiency of the training results reduced the complexity of the conventional iterative scheme, as shown in Algorithm 2.

Algorithm 2 Gradient Descent with Chain Rule for DNN Training Algorithm

1- Set ɷ, Ъ, δ and $\mathfrak{S}$ randomly
2- Repeat
3- $k \leftarrow 0$, $\text{ɷ}_{old} \leftarrow \text{ɷ}$, $\text{Ъ}_{old} \leftarrow \text{Ъ}$
4- Generate ƻ
5- Compute $\mathcal{X}$ according to (25)
6- $\text{ɷ}_{new} \leftarrow \text{ɷ}_{old} - \delta \frac{\partial \text{ƀ}(\text{ɷ},\text{Ъ})}{\partial \text{ɷ}}$
7- $\text{Ъ}_{new} \leftarrow \text{Ъ}_{old} - \delta \frac{\partial \text{ƀ}(\text{ɷ},\text{Ъ})}{\partial \text{Ъ}}$
8- Derivative of the innerfor GD by applying the chain rule in (33) and (34)
9- Compute the input vector ƻ_k by applying a chain rule
10- $k \leftarrow k + 1$
11- **Until** $\left|\text{ƀ}(\text{ɷ}, \text{Ъ}) \leftarrow \text{ƀ}(\text{ɷ}_{old}, \text{Ъ}_{old})\right| < \mathfrak{S}$

where $\mathfrak{S}$ represents the iteration continued $\text{ƀ}(\text{ɷ}, \text{Ъ})$ was less than $\mathfrak{S} = 10^{-4}$.

V. SIMULATION RESULTS

This section provides numerical results that evaluated the effectiveness of our proposed DNN based on joint TX precoding and IoT PS designs that incorporated MISO SWIPT system using simulation parameters Table 1. One computer node with two 8-core Intel Haswell processors, two Nvidia K20 Graphical Processing Units (GPUs), and 128 GB of RAM is used to construct the suggested DNN technique using Python 3.6.0 and MATLAB.

While not used during testing, GPUs are utilized during training to shorten training times. The average channel loss at a unit reference distance $d_k^{-\alpha}$ was TX to RX_k, and α was the exponent of path loss. The K RXs and TX were placed uniformly over a square field and at its center, respectively. Then, we compared it with the results of the linear EH model shown in [38] and [41].

A. ENERGY HARVESTING VS NUMBER OF IoT DEVICES

The values of the loss function against the number of iterations for the training learning rate are shown in Fig. 3.

TABLE 1. Simulation parameters.

parameter	value
Maximum power p_k^{max}	26 dBm
Power consumption $\mathrm{P}_{\mathrm{conv}}$	20 dm
Number of IoT devices K	10
Number of antennas at the base station N	16
Carrier frequency / Channel bandwidth $\mathbb{W}$	2.45GHz/180kHz
EH efficiency factor ϑ	0.5
Noise power σ_n^2	−104 dBm/Hz
Required EH $\mathbb{E}_{min}$	-10 dm
Path loss exponent α	2.8
Number of layers in DNN N_l	8
Number of nodes in every hidden layer$\mathrm{N}_{\mathcal{L}}$	200
learning rate δ	0.001

The effect of the learning rate and total training duration on the loss function was assessed on the validation data for the convergence rate in Algorithm 2 regarding the Gaussian interference channel. The original value of the learning rate was 0.125. When the learning rate was reduced to 0.01, the small decay value had a lesser effect than the original setting, whereas a large decay value had a significant effect. Therefore, reducing the learning rate decreased the decay value to less than 0.07 within 1000 iterations. Following an update, the loss changed nonlinearly and was influenced by the learning rate. The gradient vanishing problem was indicated by the training process converging to a higher value of the loss function for learning rates δ between 0.0010 and 0.0020. The optimization became unstable when the learning rate exceeded 0.0050. Fig. 4 illustrates the QoS requirement against the number of IoT devices. QoS improvements depended on maximizing the minimum harvested energy among RXs with the lowest satisfaction rate in (2) and (3) by satisfying $\mathcal{R}_k^{Tx} > \mathcal{R}_1$ and $\mathcal{R}_k^{Rx} > \mathcal{R}_2$. The QoS satisfaction of the four techniques grew monotonically as the number of IoT devices increased because every IoT device's received SINR chose a good quality of channel and ensured the desired arrival rate when p_k^{max} increased. Our proposed DNN training algorithm for chain rule had a slightly higher QoS to IoT devices, offering better performance than the reduced power and OTPR algorithms. For all interference link distances, the DNN training for chain rule could also obtain comparable performance to that of the ES. Additionally, DNN training outperformed OTPR because it used chain rule approaches to learn in a dynamic environment, and base stations with higher transmission power generated more energy for IoT devices to harvest and satisfy their QoS requirements.

From Fig. 5, the EE declines when the number of IoT devices increases. However, the EE value curve declined more steeply for the reduced power [41] and the OTPR approaches at the increased number of devices due to increased interference. In addition, the EE enhancement offered by the larger-than-harvested energy cannot compensate for the EE loss. Moreover, the transmission power and co-channel assignment must be carefully tuned to correct $\mathcal{P}_k$ and ξ_k in interference-limited situations to prevent the EE performance from decreasing. Our proposed DNN training

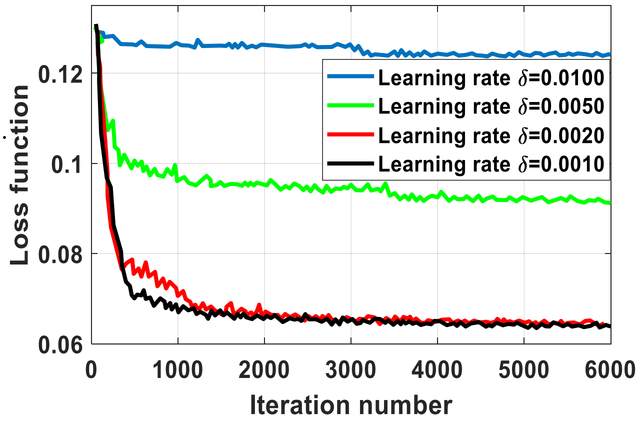

FIGURE 3. Learning rate selection for Gaussian interference channel case, K = 30.

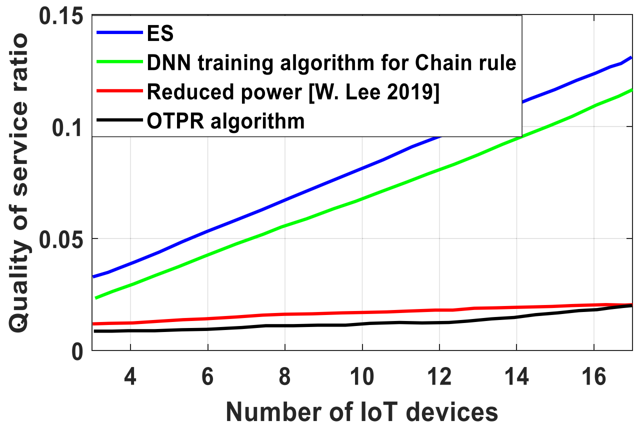

FIGURE 4. Quality of service versus the number of IoT devices.

algorithm provided a high EE by applying the chain rule to update the training, avoided the training failure to decrease the loss function at every training, and optimized the global co-channel. Although the ES produced high EE, it was a time-consuming technique due to the realistic system models for users and numerous co-channels. The ES improved EE by about 3.26%, 100.52%, and 123.90% compared to the DNN training algorithm for the chain rule, reduced power [41], and the OTPR algorithms, respectively. Fig. 6, shows increasing the number of IoT devices from 10 to 22 led to a lower propagation loss for RF power for EH. However, the TX burden to transmit energy to more RXs increased by K = 10 RXs, considerably declining the $\mathcal{P}_k^*$. The effect of the nonlinear rectification efficiency ϑ on the optimized harvested DC power $\mathbb{E}_k = \vartheta \mathcal{P}_k^*$ when each RX's RF EH unit was the power cast P1110 EVB [42] showed that the RF power for EH had a decreasing trend that got worse as K became higher.

From the proposed algorithms, the received RF power for EH obtained using the proposed DNN training for the chain rule TX precoding design, the reduced power [41], and the OTPR of the concatenated channel matrix for all RXs displayed a mean 4.2 dBm performance reduction. Moreover, the EH performed incredibly poorly in terms of EH performance to maximize the total RF power. Therefore, it was concluded that the DNN training algorithm for the chain rule for joint TX precoding and IoT PS design significantly improved the existing competitive ES schemes.

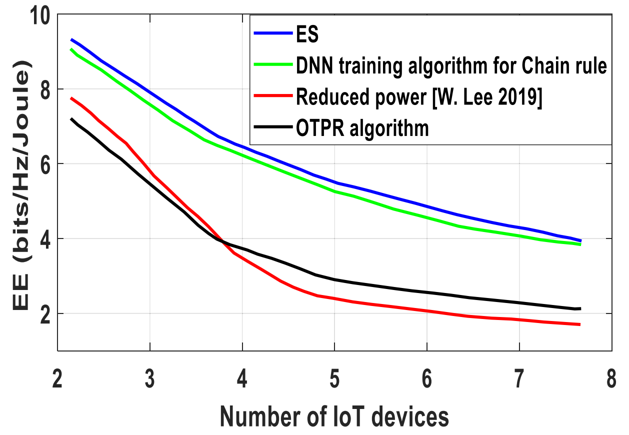

FIGURE 5. EE versus the number of IoT devices.

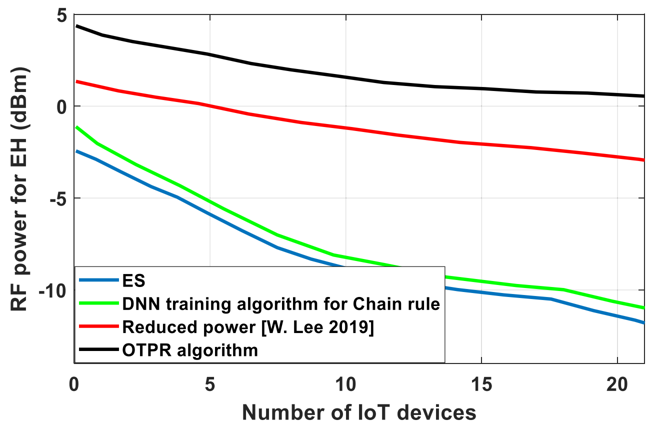

FIGURE 6. RF power versus the number of IoT devices.

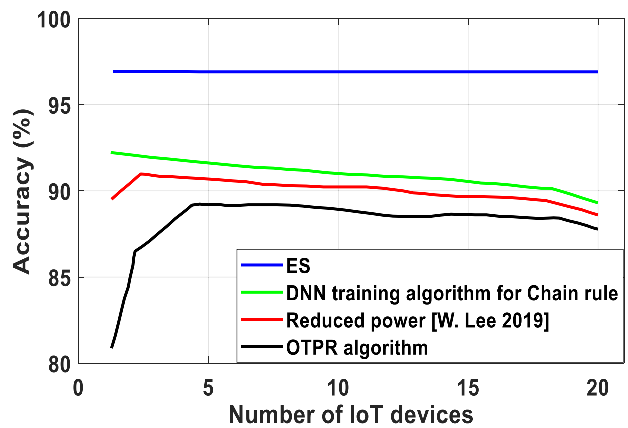

FIGURE 7. Accuracy versus the number of IoT devices.

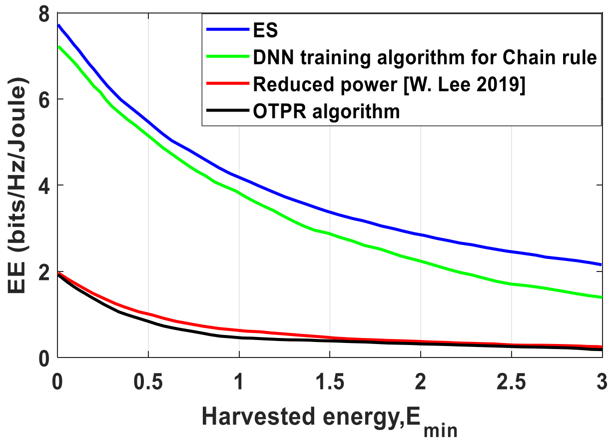

FIGURE 8. EE versus harvesting energy.

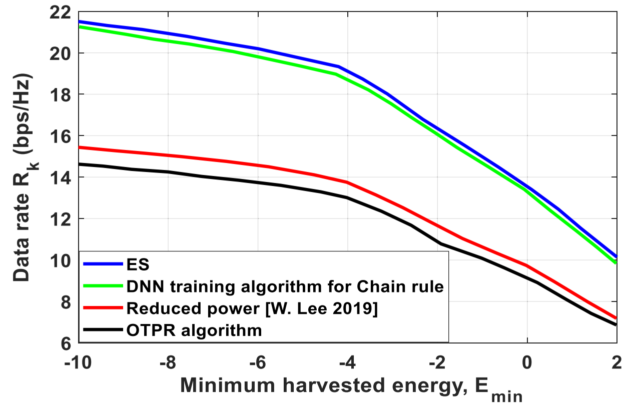

FIGURE 9. Data rate versus minimum harvested energy.

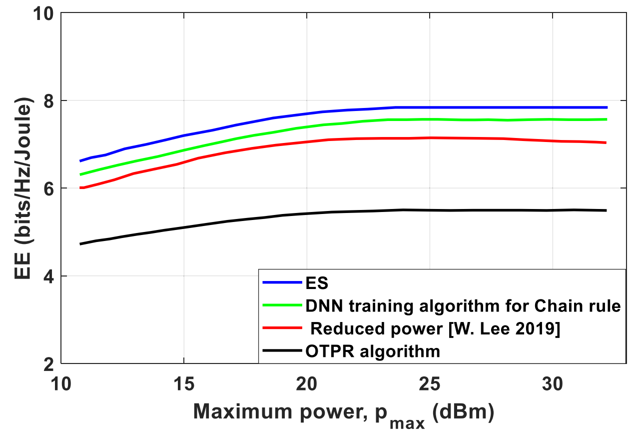

FIGURE 10. EE versus maximum transmit power.

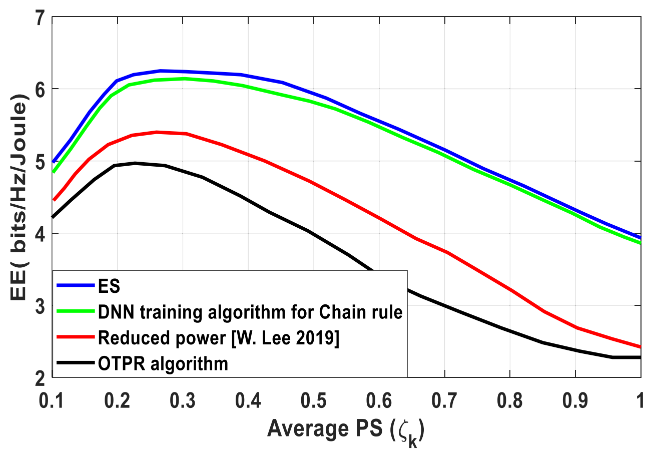

FIGURE 11. EE versus average PS.

However, reduced power [41] and OTPR algorithm TX precoding designs yielded significant energy savings. Fig. 7, shows the highest achievable accuracy versus the number of IoT devices. From Fig. 7, the activation function, such as sigmoid and ReLU, for the DNN training a chain rule provided higher accuracy than reduced power [41] and OTPR. It was because a larger training of the ES model had a higher statistical power to achieve higher accuracy and provided the best RA accuracy in the regression of optimal $\mathcal{P}_k$ and ξ_k against channel gains. The accuracy for ES was greater than 95%, higher than the other algorithms. The ES accuracy remained consistent with the increased number of IoT devices. In contrast, the accuracy dropped for the three algorithms due to their inability to optimize the minimum harvested energy for large interference power.

B. EE VS EH

Fig. 8, shows the effects of the minimal harvested energy requirements with the EE. The EE decreased for all schemes. It was due to the longer time required by each IoT device for EH to fulfill the rising minimum harvested energy requirement. Satisfying EH requirements and optimizing TX precoding and PS operation take a shorter time for ID, resulting in lower data rates. Furthermore, the DNN training for chain rule provides a near-optimal performance EE with less computation time than an ES but with the shortest training time. In addition, the OTPR provides the same performance EE for reduced power [41] because the performance of the OTPR algorithm adopts the weighted EEs of individual IoT devices and selects a minimized total energy consumption under maximizing the minimum harvested power.

Fig. 9, shows the impact of the performances of the four algorithms in different system environments in terms of the data rate and minimum harvested energy $\mathbb{E}_{min}$. The DNN could not be trained to effectively approximate the best solution based on the direct adaptation of the optimization problem (9) to the loss function (Ⱡ (Ѡ, Ъ) (30). According to (30), enhancing the learning depends on minimizing the loss function for the interference of the channel and achieving the optimal RC to obtain a high data rate. The DNN for the chain rule approaches had comparable performances to the ES for low $\mathbb{E}_{min}$. It was observed that as $\mathbb{E}_{min}$ increased, the data rate decreased. It was because more powers must be assigned to EH IoT devices, with poor channel conditions in a very deep fade when $\mathbb{E}_{min}$ is high to meet the minimum harvesting need.

C. EE VS POWER

Fig. 10, shows the performance of EE with maximum transmit power. The maximum transmitted power p_k^{max} grew for all algorithms (ES, DNN training for chain rule, reduced power, and OTPR schemes). The EE increased when the transmit power values were initially small values. However, when the transmitting power increased, and P_{max} rose to a maximum of 25 dBm, the energy dissipation increased. The usage of additionally transmitted power, p_k^{max}, above 25 dBm, resulted in a loss of EE due to the significantly increased energy dissipation rate. The proposed DNN training of the chain rule-based approach outperformed the reduced power and OTPR schemes and achieved a performance close to that of the ES in every environment. The chain rules of the DNN training approach could efficiently optimize the problem of the cost function (30) and train the neural network to approximate the best solution. Therefore, the DNN training algorithm for the chain rule maximizes the EE more than reduced power and OTPR schemes, according to the changes in p_k^{max} and ϑ. From Fig. 11, the minimum harvested energy requirement has an impact on EE. The EE worsened when the minimum harvested energy demand increased when $\xi_k \in [0.2 < x < 0.4]$ for $k \in \mathbb{K}$. It occurred because the RF signals to the harvested energy were unpredictable due to the stochastic nature of energy sources and extra energy consumption for devices with different power levels. The EE increased with the PS ratio when ξ_k was small. The DNN training showed near-optimal EE performances for all algorithm converges by minimizing unneeded label data with the lower PS ratio value. These observations illustrated the near optimality of the DNN training for chain rule because the DNN outcomes were significantly closer to ES than OTPR.

VI. CONCLUSION

This work proposed RA for the OTPR algorithm to regulate transmission power to maximize the EE for SWIPT. We also proposed a DNN training for chain rule algorithm to solve distributed non-convex and NP-hardness caused by co-channel interference to reduce the loss and maximize the EE performance. The proposed DNN to avoid training failure was based on the chain rule for the GD algorithm for FNN training to increase the output accuracy and reduce the loss. The DNN training for chain rule optimized the global co-channel interference in IoT networks. It also provided a near-optimal performance EE with less computation time than an ES with the shortest training time. Edge artificial intelligence is implementing machine learning models, such as DNNs, directly on edge computing nodes or IoT devices instead of depending exclusively on cloud platforms or centralized servers for data processing and analysis. The IoT has grown thanks to Edge Computing (EC) with artificial intelligence-EH technologies, which enable various IoT devices to be interconnected in future work to guide IoT EH devices in choosing offloading rates and EC devices based on predicted energy and battery levels.

REFERENCES

[1] H. Rahmani, D. Shetty, M. Wagih, Y. Ghasempour, V. Palazzi, N. B. Carvalho, R. Correia, A. Costanzo, D. Vital, F. Alimenti, J. Kettle, D. Masotti, P. Mezzanotte, L. Roselli, and J. Grosinger, "Next-generation IoT devices: Sustainable eco-friendly manufacturing, energy harvesting, and wireless connectivity," *IEEE J. Microw.*, vol. 3, no. 1, pp. 237–255, Jan. 2023.

[2] Z. Yang, W. Xu, Y. Pan, C. Pan, and M. Chen, "Energy efficient resource allocation in machine-to-machine communications with multiple access and energy harvesting for IoT," *IEEE Internet Things J.*, vol. 5, no. 1, pp. 229–245, Feb. 2018.

[3] Z. Ni, R. V. Bhat, and M. Motani, "On dual-path energy-harvesting receivers for IoT with batteries having internal resistance," *IEEE Internet Things J.*, vol. 5, no. 4, pp. 2741–2752, Aug. 2018.

[4] P. Kamalinejad, C. Mahapatra, Z. Sheng, S. Mirabbasi, V. C. M. Leung, and Y. L. Guan, "Wireless energy harvesting for the Internet of Things," *IEEE Commun. Mag.*, vol. 53, no. 6, pp. 102–108, Jun. 2015.

[5] B. Clerckx, "Wireless information and power transfer: Nonlinearity, waveform design, and rate-energy tradeoff," *IEEE Trans. Signal Process.*, vol. 66, no. 4, pp. 847–862, Feb. 2018.

[6] R. Jiang, K. Xiong, P. Fan, L. Zhou, and Z. Zhong, "Outage probability and throughput of multirelay SWIPT-WPCN networks with nonlinear EH model and imperfect CSI," *IEEE Syst. J.*, vol. 14, no. 1, pp. 1206–1217, Mar. 2020.

[7] T. D. Nguyen, J. Y. Khan, and D. T. Ngo, "A self-sustainable RF energy harvesting algorithm for WSN-based IoT applications," in *Proc. GLOBECOM IEEE Global Commun. Conf.*, Dec. 2017, pp. 1–6.

[8] X. Liu, Z. Qin, Y. Gao, and J. A. McCann, "Resource allocation in wireless powered IoT networks," *IEEE Internet Things J.*, vol. 6, no. 3, pp. 4935–4945, Jun. 2019.

[9] A. Rauniyar, P. E. Engelstad, and O. N. Østerbø, "Performance analysis of RF energy harvesting and information transmission based on NOMA with interfering signal for IoT relay systems," *IEEE Sensors J.*, vol. 19, no. 17, pp. 7668–7682, Sep. 2019.

[10] K. Lee, J.-P. Hong, H. Seo, and W. Choi, "Learning-based resource management in device-to-device communications with energy harvesting requirements," *IEEE Trans. Commun.*, vol. 68, no. 1, pp. 402–413, Jan. 2020.

[11] Z. Masood, H. Park, H. S. Jang, S. Yoo, S. P. Jung, and Y. Choi, "Optimal power allocation for maximizing energy efficiency in DAS-based IoT network," *IEEE Syst. J.*, vol. 15, no. 2, pp. 2342–2348, Jun. 2021.

[12] M. Chu, B. He, X. Liao, Z. Gao, and V. C. M. Leung, "On the design of power splitting relays with interference alignment," *IEEE Trans. Commun.*, vol. 66, no. 4, pp. 1411–1424, Apr. 2018.

[13] M. Sheng, L. Wang, X. Wang, Y. Zhang, C. Xu, and J. Li, "Energy efficient beamforming in MISO heterogeneous cellular networks with wireless information and power transfer," *IEEE J. Sel. Areas Commun.*, vol. 34, no. 4, pp. 954–968, Apr. 2016.

[14] Q. Shi, L. Liu, W. Xu, and R. Zhang, "Joint transmit beamforming and receive power splitting for MISO SWIPT systems," *IEEE Trans. Wireless Commun.*, vol. 13, no. 6, pp. 3269–3280, Jun. 2014.

[15] D. Mishra and S. De, "Utility maximization models for two-hop energy relaying in practical RF harvesting networks," in *Proc. IEEE Int. Conf. Commun. Workshops (ICC Workshops)*, Paris, France, May 2017, pp. 41–46.

[16] Z. Zhu, N. Wang, W. Hao, Z. Wang, and I. Lee, "Robust beamforming designs in secure MIMO SWIPT IoT networks with a nonlinear channel model," *IEEE Internet Things J.*, vol. 8, no. 3, pp. 1702–1715, Feb. 2021.

[17] A. Omidkar, A. Khalili, H. H. Nguyen, and H. Shafiei, "Reinforcement-learning-based resource allocation for energy-harvesting-aided D2D communications in IoT networks," *IEEE Internet Things J.*, vol. 9, no. 17, pp. 16521–16531, Sep. 2022.

[18] Z. Shi, X. Xie, H. Lu, H. Yang, J. Cai, and Z. Ding, "Deep reinforcement learning-based multidimensional resource management for energy harvesting cognitive NOMA communications," *IEEE Trans. Commun.*, vol. 70, no. 5, pp. 3110–3125, May 2022.

[19] H. Sun, X. Chen, Q. Shi, M. Hong, X. Fu, and N. D. Sidiropoulos, "Learning to optimize: Training deep neural networks for interference management," *IEEE Trans. Signal Process.*, vol. 66, no. 20, pp. 5438–5453, Oct. 2018.

[20] J. J. Park, J. H. Moon, K.-Y. Lee, and D. I. Kim, "Transmitter-oriented dual-mode SWIPT with deep-learning-based adaptive mode switching for IoT sensor networks," *IEEE Internet Things J.*, vol. 7, no. 9, pp. 8979–8992, Sep. 2020.

[21] W. Lee, K. Lee, H.-H. Choi, and V. C. M. Leung, "Deep learning for SWIPT: Optimization of transmit-harvest-respond in wireless-powered interference channel," *IEEE Trans. Wireless Commun.*, vol. 20, no. 8, pp. 5018–5033, Aug. 2021.

[22] D. P. Kingma and J. Ba, "Adam: A method for stochastic optimization," in *Proc. Int. Conf. Learn. Represent.*, San Diego, CA, USA, May 2015, pp. 1–15.

[23] L. Bottou, "Large-scale machine learning with stochastic gradient descent," in *Proc. COMPSTAT*, Paris France. Cham, Switzerland: Springer, 2010, pp. 177–186.

[24] I. Goodfellow, Y. Bengio, A. Courville, and Y. Bengio, *Deep Learning*. Cambridge, MA, USA: MIT Press, 2016.

[25] M. Mohammadi, A. Al-Fuqaha, S. Sorour, and M. Guizani, "Deep learning for IoT big data and streaming analytics: A survey," *IEEE Commun. Surveys Tuts.*, vol. 20, no. 4, pp. 2923–2960, 4th Quart., 2018.

[26] K. I. Ahmed, H. Tabassum, and E. Hossain, "Deep learning for radio resource allocation in multi-cell networks," *IEEE Netw.*, vol. 33, no. 6, pp. 188–195, Nov. 2019.

[27] D. Mishra, G. C. Alexandropoulos, and S. De, "Energy sustainable IoT with individual QoS constraints through MISO SWIPT multicasting," *IEEE Internet Things J.*, vol. 5, no. 4, pp. 2856–2867, Aug. 2018.

[28] B. C. Chung, K. Lee, and D.-H. Cho, "Proportional fair energy-efficient resource allocation in Energy-Harvesting-Based wireless networks," *IEEE Syst. J.*, vol. 12, no. 3, pp. 2106–2116, Sep. 2018.

[29] A. Salh, R. Ngah, G. A. Hussain, L. Audah, M. Alhartomi, Q. Abdullah, R. Alsulami, S. Alzahrani, and A. Alzahmi, "Intelligent resource management using multiagent double deep Q-networks to guarantee strict reliability and low latency in IoT network," *IEEE Open J. Commun. Soc.*, vol. 3, pp. 2245–2257, 2022.

[30] X. Zhou, R. Zhang, and C. K. Ho, "Wireless information and power transfer: Architecture design and rate-energy tradeoff," *IEEE Trans. Commun.*, vol. 61, no. 11, pp. 4754–4767, Nov. 2013.

[31] L. Liu, R. Zhang, and K.-C. Chua, "Wireless information and power transfer: A dynamic power splitting approach," *IEEE Trans. Commun.*, vol. 61, no. 9, pp. 3990–4001, Sep. 2013.

[32] X. Lu, P. Wang, D. Niyato, D. I. Kim, and Z. Han, "Wireless networks with RF energy harvesting: A contemporary survey," *IEEE Commun. Surveys Tuts.*, vol. 17, no. 2, pp. 757–789, 2nd Quart., 2015.

[33] R. C. Qiu, Z. Hu, H. Li, and M. C. Wicks, "Convex optimization," in *Cognitive Radio Communication and Networking: Principles and Practice*. Cambridge, U.K.: Cambridge Univ. Press, 2013, pp. 235–282.

[34] Z.-Q. Luo and S. Zhang, "Dynamic spectrum management: Complexity and duality," *IEEE J. Sel. Topics Signal Process.*, vol. 2, no. 1, pp. 57–73, Feb. 2008.

[35] R. M. Corless, G. H. Gonnet, D. E. G. Hare, D. J. Jeffrey, and D. E. Knuth, "On the Lambert W function," *Adv. Comput. Math.*, vol. 5, no. 1, pp. 329–359, 1996.

[36] J. Fliege, A. I. F. Vaz, and L. N. Vicente, "Complexity of gradient descent for multiobjective optimization," *Optim. Methods Softw.*, vol. 34, no. 5, pp. 949–959, Aug. 2018.

[37] T.-V. Nguyen, T.-N. Tran, K. Shim, T. Huynh-The, and B. An, "A deep-neural-network-based relay selection scheme in wireless-powered cognitive IoT networks," *IEEE Internet Things J.*, vol. 8, no. 9, pp. 7423–7436, May 2021.

[38] H. Yang, Y. Ye, X. Chu, and M. Dong, "Resource and power allocation in SWIPT-enabled device-to-device communications based on a nonlinear energy harvesting model," *IEEE Internet Things J.*, vol. 7, no. 11, pp. 10813–10825, Nov. 2020.

[39] W. Lee, M. Kim, and D.-H. Cho, "Deep power control: Transmit power control scheme based on convolutional neural network," *IEEE Commun. Lett.*, vol. 22, no. 6, pp. 1276–1279, Jun. 2018.

[40] Z. Zhang, Y. Lu, Y. Huang, and P. Zhang, "Neural network-based relay selection in two-way SWIPT-enabled cognitive radio networks," *IEEE Trans. Veh. Technol.*, vol. 69, no. 6, pp. 6264–6274, Jun. 2020.

[41] W. Lee, T.-W. Ban, and B. C. Jung, "Distributed transmit power optimization for device-to-device communications underlying cellular networks," *IEEE Access*, vol. 7, pp. 87617–87633, 2019.

[42] *Powercast*. Accessed: Feb. 2023. [Online]. Available: http://www.powercastco.com

SAEED ALZAHRANI (Member, IEEE) received the B.S. degree from King Abdulaziz University, Jeddah, Saudi Arabia, the M.S. degree from the University of Colorado at Colorado Springs, and the Ph.D. degree from The Ohio State University, all in electrical engineering. He was with the Microelectronics Research Laboratory, University of Colorado at Colorado Springs, from 2012 to 2014, involved in developing tunable ferroelectric-based filters, VCOs, amplifiers, and antennas. From 2014 to 2019, he was with the ElectroScience Laboratory, The Ohio State University, focusing on developing design techniques for wide TR VCOs at mm-wave frequency band. He is currently an Assistant Professor with the Electrical Engineering Department, University of Tabuk, Saudi Arabia. His research interests include addresses design and technological challenges related to RF/millimeter-wave and mixed-signal integrated circuits and systems for emerging technologies, including communication, automotive, and biomedical applications.

ADEB SALH received the bachelor's degree in electrical and electronic engineering from IBB University, Yemen, in 2007, and the master's and Ph.D. degrees in electrical and electronic engineering from Universiti Tun Hussein Onn Malaysia (UTHM), in 2015 and 2020, respectively. From 2007 to 2012, he was a Lecturer Assistant with the Yareem Community College. From 2020 to 2023, he was a Postdoctoral Researcher with UTHM and UTM, respectively. Currently, he is an Assistant Professor with the Faculty of Information and Communication Technology, Universiti Tunku Abdul Rahman. His research interests include 5G, 6G wireless communications, massive MIMO, artificial intelligence (AI), and the Internet of Things (IoT).

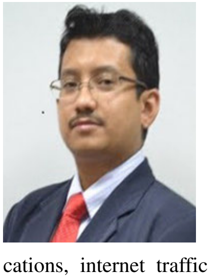

LUKMAN AUDAH (Member, IEEE) received the Bachelor of Engineering degree in telecommunications from Universiti Teknologi Malaysia, in 2005, and the M.Sc. degree in communication networks and software and the Ph.D. degree in electronic engineering from the University of Surrey, U.K. He is currently a Senior Lecturer with the Communication Engineering Department, Universiti Tun Hussein Onn Malaysia. His research interests include wireless and mobile communications, internet traffic engineering, network system management, data security, and satellite communications.

MOHAMMED A. ALHARTOMI (Member, IEEE) received the B.Sc. degree from King Abdulaziz University, Jeddah, Saudi Arabia, the M.Sc. degree from Swansea University, Swansea, U.K., with a focus on wireless communications systems, and the Ph.D. degree from the University of Leeds, Leeds, U.K., in 2016. He is an Associate Professor with the Electrical Engineering Department, University of Tabuk, Saudi Arabia. He is also a Visiting Scholar with the University of Central Florida, working on dense VLC networks. His research interests include mobile and wireless communications, optical communications, and signal processing.

ABDULAZIZ ALOTAIBI received the B.Eng. degree in electrical engineering and the M.Sc. degree in systems engineering from Florida Institute of Technology, and the Ph.D. degree in manufacturing engineering from Loughborough University, U.K. He is currently an Assistant Professor with the Industrial Engineering Department, University of Tabuk, Saudi Arabia. His research interests include dynamic optimization, resource consumption minimization, agent-based distributed industrial control, and intelligent manufacturing.

RUWAYBIH ALSULAMI (Member, IEEE) was born in Makkah, Saudi Arabia. He received the B.S. degree in electrical and computer engineering from the University of Colorado at Boulder, Boulder, CO, USA, in 2011, the M.S. degree in electrical engineering from the University of Colorado at Colorado Springs, Colorado Springs, CO, in 2013, and the dual Ph.D. degrees in electrical and computer engineering from The Ohio State University, Columbus, OH, USA, in 2020 and 2021, respectively. He is currently an Assistant Professor in electrical engineering with Umm Al-Qura University, Mecca. His current research interests include circuit design, such as antennas, filters, multiband power amplifiers, PA linearization, and measurements of nonlinear microwave devices and circuits.